



Original Article



# Biomarker Discovery for Metabolic Dysfunction-associated Steatotic Liver Disease Utilizing Mendelian Randomization, Machine Learning, and External Validation

Gong Feng<sup>1</sup>, Giovanni Targher<sup>2,3</sup>, Christopher D. Byrne<sup>4</sup>, Na He<sup>5</sup>, Man Mi<sup>6</sup>, Yi Liu<sup>7</sup>, Hongbin Zhu<sup>8</sup>, Ming-Hua Zheng<sup>9,10</sup> and Feng Ye<sup>1\*</sup>

<sup>1</sup>Department of Infectious Diseases, The First Affiliated Hospital of Xi'an Jiaotong University, Xi'an, Shaanxi, China; <sup>2</sup>Department of Medicine, University of Verona, Verona, Italy; <sup>3</sup>Metabolic Diseases Research Unit, IRCSS Sacro Cuore-Don Calabria Hospital, Negrar di Valpolicella, Italy; <sup>4</sup>Southampton National Institute for Health and Care Research Biomedical Research Centre, University Hospital Southampton and University of Southampton, Southampton General Hospital, Southampton, UK; <sup>5</sup>Department of Gastroenterology, The First Affiliated Hospital of Xi'an Medical University, Xi'an, Shaanxi, China; <sup>6</sup>Xi'an Medical University, Xi'an, Shaanxi, China; <sup>7</sup>Department of Traditional Chinese Medicine, The First Affiliated Hospital of Xi'an Jiaotong University, Xi'an, Shaanxi, China; <sup>8</sup>Department of Gastroenterology, the 983rd Hospital of the Joint Logistics Support Force of the Chinese People's Liberation Army, Tianjin, China; <sup>9</sup>MAFLD Research Center, Department of Hepatology, the First Affiliated Hospital of Wenzhou Medical University, Wenzhou, Zhejiang, China; <sup>10</sup>Key Laboratory of Diagnosis and Treatment for The Development of Chronic Liver Disease in Zhejiang Province, Wenzhou, Zhejiang, China

Received: June 06, 2025 | Revised: June 22, 2025 | Accepted: July 02, 2025 | Published online: July 16, 2025

## Abstract

**Background and Aims:** The causal biomarkers for metabolic dysfunction-associated steatotic liver disease (MASLD) and their clinical value remain unclear. In this study, we aimed to identify biomarkers for MASLD and evaluate their diagnostic and prognostic significance. **Methods:** We conducted a Mendelian randomization analysis to assess the causal effects of 2,925 molecular biomarkers (from proteomics data) and 35 clinical biomarkers on MASLD. Mediation analysis was performed to determine whether clinical biomarkers mediated the effects of molecular biomarkers. The association between key clinical biomarkers and MASLD was externally validated in a hospital-based cohort (n = 415). A machine learning-based diagnostic model for MASLD was developed and validated using the identified molecular biomarkers. Prognostic significance was evaluated for both molecular and clinical biomarkers. **Results:** Six molecular biomarkers—including canopy FGF signaling regulator 4 (CNPY4), ectonucleoside triphosphate diphosphohydrolase 6 (ENTPD6), and major histocompatibility complex, class I, A (HLA-A)—and eight clinical biomarkers (e.g., serum total protein (STP)) were identified as causally related to MASLD. STP partially mediated the effect of HLA-A on MASLD (23.61%) and was associated with MASLD in the external cohort (odds ratio = 1.080, 95% confidence interval: 1.011–1.155). A random forest model demonstrated high diagnostic performance

(AUC = 0.941 in training; 0.875 in validation). High expression levels of CNPY4 and ENTPD6 were associated with the development of and poorer survival from hepatocellular carcinoma. Low STP (<60 g/L) predicted all-cause mortality (HR = 2.50, 95% confidence interval: 1.22–5.09). **Conclusions:** This study identifies six causal molecular biomarkers (e.g., CNPY4, ENTPD6, HLA-A) and eight clinical biomarkers for MASLD. Notably, STP mediates the effect of HLA-A on MASLD and is associated with all-cause mortality.

**Citation of this article:** Feng G, Targher G, Byrne CD, He N, Mi M, Liu Y, et al. Biomarker Discovery for Metabolic Dysfunction-associated Steatotic Liver Disease Utilizing Mendelian Randomization, Machine Learning, and External Validation. J Clin Transl Hepatol 2025. doi: 10.14218/JCTH.2025.00270.

## Introduction

Metabolic dysfunction-associated steatotic liver disease (MASLD) has attracted increasing attention, with a global prevalence of around 30–35%.<sup>1</sup> A recent epidemiological model prediction suggests that by 2030, the global prevalence of MASLD will rise to 36.8%, corresponding to approximately 101.2 million people. By 2050, the prevalence is expected to increase further to 41.4%, affecting approximately 122 million people.<sup>2</sup> With this rising prevalence, the disease burden of MASLD-related liver cancer has also become increasingly significant.<sup>3</sup> Globally, incident cases, deaths, and disability-adjusted life years attributable to MASLD-related liver cancer in 2019 increased by 205%, 195%, and 166%, respectively, compared with 1990.<sup>4</sup> In the United States, MASLD has become the leading cause of liver cancer among liver transplant

**Keywords:** Metabolic dysfunction-associated fatty liver disease; Mendelian randomization; Machine learning; Proteomics; Mediation analysis; Non-invasive diagnosis; Prognosis; Causal biomarkers.

\*Correspondence to: Feng Ye, Department of Infectious Diseases, The First Affiliated Hospital of Xi'an Jiaotong University, Xi'an, Shaanxi 710061, China. ORCID: <https://orcid.org/0000-0003-1418-7980>; Tel: +86-18991232860; Fax: +86-2985323533; E-mail: yefeng.jiaotong@163.com.

candidates.<sup>5</sup>

Despite growing awareness of MASLD, the causal biomarkers underlying this condition remain unclear.<sup>6</sup> Identifying such biomarkers has become an urgent research priority. As an effective tool for causal inference, Mendelian randomization (MR) can reduce confounding and reverse causation biases inherent in observational studies by using genetic variations as instrumental variables, thereby providing more robust evidence for causal relationships between diseases and related factors.<sup>7,8</sup> Although some studies have applied MR to investigate genetic susceptibility and potential biomarkers for MASLD, most published research has focused on a limited number of biomarkers, lacking a systematic and comprehensive approach.<sup>9,10</sup>

Biomarkers related to MASLD include not only traditional clinical biomarkers but also novel molecular biomarkers identified through multi-omics technologies.<sup>11</sup> Clinical biomarkers, as standard medical indicators, are widely used for disease diagnosis, prognostic assessment, and therapeutic monitoring due to their accessibility and established clinical utility.<sup>11</sup> In contrast, molecular biomarkers reflect the underlying mechanisms of disease development and progression and are typically derived from multi-omics platforms such as transcriptomics and proteomics.<sup>11,12</sup> Although many biomarkers associated with MASLD have been identified, their clinical significance remains insufficiently characterized.<sup>13</sup> When used collectively, these biomarkers have the potential to improve the accuracy of noninvasive MASLD diagnosis, thereby reducing the need for liver biopsies.<sup>14,15</sup> Moreover, they may serve as prognostic indicators; for example, the novel acMASH index has been shown to correlate with all-cause mortality risk and assist in risk stratification.<sup>16</sup> Therefore, understanding the clinical and translational relevance of biomarkers with a confirmed causal relationship to MASLD is critically important.

In this study, we aimed to identify causal molecular biomarkers (based on proteomics data) and clinical biomarkers associated with MASLD, and to evaluate their diagnostic and prognostic significance. First, we conducted MR analysis to assess the causal effects of 2,925 molecular biomarkers and 35 clinical biomarkers on MASLD, thereby revealing the causal relationships between these biomarkers and MASLD. Mediation analysis was performed to determine whether key clinical biomarkers mediated the effects of molecular biomarkers (exposures) on MASLD (the outcome). The association between key clinical biomarkers and MASLD was also externally validated in a hospital-based cohort. Second, we applied six machine-learning algorithms to develop and validate a novel noninvasive diagnostic model for MASLD based on the identified molecular biomarkers. Third, we explored the prognostic value of molecular biomarkers for the development of and poorer survival from hepatocellular carcinoma (HCC) using data from The Cancer Genome Atlas. We also assessed the prognostic significance of key clinical biomarkers for all-cause mortality and cause-specific mortality by analyzing prospective data from the National Health and Nutrition Examination Survey (NHANES).

## Methods

### **Data collection of molecular and clinical biomarkers and MASLD for MR analysis**

In this study, the molecular biomarkers were derived from proteomics data obtained from the FinnGen database.<sup>17</sup> This database included 619 samples encompassing 2,925 mole-

cules, such as apolipoprotein E (APOE), canonical FGF signaling regulator 4 (CNPY4), ectonucleoside triphosphate diphosphohydrolase 6 (ENTPD6), major histocompatibility complex, class I, A (HLA-A), secretogranin III (SCG3), and torsin 1A interacting protein 1 (TOR1AIP1), which were publicly released in April 2024.<sup>17</sup> Our clinical biomarkers comprised 35 blood and urine biomarkers from the UK Biobank dataset, which included 363,228 individuals.<sup>18</sup> These 35 biomarkers are extensively utilized in clinical diagnostics and contribute to assessing various physiological functions, including serum albumin, APOE, gamma-glutamyl transferase (GGT), high-density lipoprotein cholesterol (HDL-C), insulin-like growth factor 1 (IGF-1), total protein, triglycerides, and urinary sodium. Data on MASLD were derived from a meta-analysis of genome-wide association studies (GWAS) involving four cohorts with electronic health record–documented MASLD among participants of European ancestry (8,434 cases and 770,180 controls).<sup>19</sup>

### **Instrumental variable screening and MR analysis**

We referred to prior literature for the screening criteria of instrumental variables (IVs) (Supplementary Method 1).<sup>20</sup> For example, in selecting IVs for the 35 clinical biomarkers, single-nucleotide polymorphisms (SNPs) were selected based on genome-wide significance ( $P < 5 \times 10^{-8}$ ) and were subsequently clumped to ensure independence using a linkage disequilibrium threshold of  $r^2 < 0.001$  within a 10,000-kb distance. A two-step, two-sample MR approach was employed to assess the causal relationships between molecular biomarkers and MASLD, as well as between clinical biomarkers and MASLD. This approach is a genetics-based method for causal inference, conducted through two independent sample datasets in two stages. In the first step, GWAS was used to identify genetic variants (such as SNPs) significantly associated with the exposure factor in the initial sample, thereby establishing a strong link between these variants and the exposure.<sup>20</sup> In the second step, these instrumental variables were tested for association with disease outcomes in a second, independent sample using statistical models, such as the inverse-variance weighted (IVW) method, while conducting heterogeneity and pleiotropy tests to validate the plausibility of the causal hypothesis.<sup>20</sup> To ensure the reliability of the MR results, we conducted heterogeneity, pleiotropy, and sensitivity analyses (Supplementary Method 2). All MR analyses employed the IVW method as the primary test for causal associations, and results were verified using the MR-Egger, weighted median, weighted mode, and simple mode methods. Since the IVW method served as the main causal association test, we corrected IVW results using the false discovery rate method;  $P_{\text{fdr}} < 0.05$  was considered statistically significant. For other analyses without false discovery rate adjustment, a  $P$ -value  $< 0.05$  was considered indicative of statistical significance.

### **Mediation effect analysis to identify key clinical biomarkers with a mediating role**

Mediation effect analysis was used to determine whether key clinical biomarkers mediated the causal relationship between molecular biomarkers and MASLD. The formulas for calculating each effect size were as follows: total effect =  $C \times 100\%$ , indirect effect =  $A \times B \times 100\%$ , direct effect ( $C'$ ) =  $[C - (A \times B) \times 100\%]$ , and the proportion of the mediation effect =  $(A \times B) / C \times 100\%$ . Among them, A is the  $\beta_1$  value of the MR analysis between the key protein and the clinical marker; B is the  $\beta_2$  value of the MR analysis between the clinical marker and MASLD; and C is the  $\beta$  value of the MR analysis between the key protein and MASLD.

### **Validation of the association between key clinical biomarkers and MASLD**

Through mediation analyses, we identified key clinical biomarkers that mediate the effects of molecular biomarkers on MASLD. To further validate externally the association between these biomarkers and MASLD, we utilized a follow-up cohort of MASLD patients from the First Affiliated Hospital of Xi'an Medical University who had undergone vibration-controlled transient elastography examinations.<sup>20</sup> Patients with a controlled attenuation parameter value  $\geq 248$  dB/m, as assessed by FibroScan, were considered to have hepatic steatosis (Supplementary Method 3).<sup>21</sup>

### **Machine learning (ML) algorithms for MASLD based on the identified molecular biomarkers**

We employed six widely used ML algorithms—including Extreme Gradient Boosting (XGBoost), Random Forest (RF), K-Nearest Neighbors (KNN), Support Vector Machine, Multilayer Perceptron, and Light Gradient Boosting Machine—to develop a noninvasive diagnostic model for MASLD. Expression profiles of the identified molecular biomarkers were obtained from the Gene Expression Omnibus database, with GSE89632 ( $n = 63$ ) serving as the training set and GSE48452 ( $n = 73$ ) as the external validation cohort.

### **Evaluation of the prognostic significance of the identified molecular and clinical biomarkers**

We further evaluated the prognostic value of the identified molecular biomarkers, particularly their impact on HCC development and overall survival (Supplementary Method 4). To investigate associations between clinical biomarkers and the risk of all-cause and cause-specific mortality, we analyzed prospective data from NHANES collected between 1999 and 2006 (Supplementary Method 5). The study design is illustrated in Figure 1.

## **Results**

### **Molecular biomarkers causally related to MASLD**

The IVW algorithm indicated that among the 2,925 molecular biomarkers, only six exhibited a significant relationship with MASLD (Fig. 2A). The mean F-statistics for the selected IVs were as follows: APOE ( $F = 36.919$ ), CNPY4 ( $F = 26.539$ ), ENTPD6 ( $F = 43.279$ ), HLA-A ( $F = 38.635$ ), SCG3 ( $F = 30.938$ ), and TOR1AIP1 ( $F = 48.678$ ). These values were well above the threshold of 10, indicating that all the IVs were strong instruments. The IVW algorithm showed that the odds ratio (OR) for APOE was 1.057 (95% confidence interval (CI): 1.031–1.083,  $P_{\text{fdr}} = 4.62\text{E-}03$ ), for CNPY4 was 1.054 (95% CI: 1.029–1.081,  $P_{\text{fdr}} = 8.38\text{E-}03$ ), for ENTPD6 was 1.031 (95% CI: 1.016–1.045,  $P_{\text{fdr}} = 5.75\text{E-}03$ ), for HLA-A was 0.969 (95% CI: 0.960–0.979,  $P_{\text{fdr}} = 1.81\text{E-}06$ ), for SCG3 was 0.956 (95% CI: 0.937–0.975,  $P_{\text{fdr}} = 4.62\text{E-}03$ ), and for TOR1AIP1 was 0.964 (95% CI: 0.950–0.979,  $P_{\text{fdr}} = 8.13\text{E-}04$ ). Results from the other four algorithms are shown in Supplementary Table 1. The Cochran's Q test analysis revealed no heterogeneity in the results for APOE, CNPY4, ENTPD6, HLA-A, SCG3, and TOR1AIP1 (Supplementary Table 2). Subsequently, the MR-Egger intercept test was conducted to evaluate the presence of pleiotropy among the IVs (Supplementary Table 2). The results indicated no horizontal pleiotropy between these six biomarkers and MASLD (Supplementary Table 2). The leave-one-out sensitivity analysis confirmed that the relationship between TOR1AIP1 and MASLD remained

stable (Fig. 2B). From the scatter plots, the relationship between TOR1AIP1 and MASLD showed a consistent trend (with OR values all greater than 1) across the five MR algorithms, further supporting the robustness of our findings (Fig. 2C). Scatter plots and leave-one-out sensitivity analyses for the remaining five proteins are detailed in Supplementary Figures 1–5. The reverse MR analysis found no significant association between MASLD and these six proteins.

### **Clinical biomarkers causally related to MASLD**

The IVW algorithm indicated that among the 35 clinical biomarkers, only eight exhibited a significant relationship with MASLD (Fig. 3A). The mean F-statistics for the selected IVs were as follows: albumin ( $F = 73.095$ ), ApoA ( $F = 135.563$ ), GGT ( $F = 129.355$ ), HDL-C ( $F = 145.250$ ), IGF-1 ( $F = 98.572$ ), urinary sodium ( $F = 40.886$ ), total protein ( $F = 63.070$ ), and triglycerides ( $F = 147.741$ ). All these values exceeded the threshold of 10, indicating that the IVs were strong instruments. The IVW algorithm revealed that the OR for albumin was 1.373 (95% CI: 1.140–1.654,  $P_{\text{fdr}} = 4.11\text{E-}03$ ), for ApoA was 0.811 (95% CI: 0.695–0.946,  $P_{\text{fdr}} = 0.026$ ), for GGT was 1.281 (95% CI: 1.167–1.406,  $P_{\text{fdr}} = 1.25\text{E-}06$ ), for HDL-C was 0.792 ( $P_{\text{fdr}} = 7.53\text{E-}05$ ), for IGF-1 was 0.870 (95% CI: 0.784–0.964,  $P_{\text{fdr}} = 0.027$ ), for urinary sodium was 2.583 (95% CI: 1.407–4.743,  $P_{\text{fdr}} = 8.548\text{E-}03$ ), for total protein was 1.248 (95% CI: 1.083–1.438,  $P_{\text{fdr}} = 8.488\text{E-}03$ ), and for triglycerides was 1.392 (95% CI: 1.239–1.563,  $P_{\text{fdr}} = 2.15\text{E-}07$ ). The MR-Egger intercept test demonstrated no horizontal pleiotropy between any of these biomarkers and MASLD. The scatter plots indicated that the relationship between total protein and MASLD exhibited a consistent trend (with OR values all greater than 1) across the five MR algorithms, further supporting the robustness of the findings (Fig. 3B). Additionally, a Manhattan plot was used to display the distribution characteristics of SNPs for total protein after removing linkage disequilibrium (Fig. 3C). Scatter plots for the other seven clinical biomarkers are shown in Supplementary Figures 6–9.

### **Total protein demonstrated a significant mediating effect in the relationship between HLA-A and MASLD**

Before conducting the mediation analysis, we used an MR approach to explore the causal relationships between the six molecular biomarkers (exposures) and the eight clinical biomarkers (outcomes), which served as a prerequisite for the mediation analysis. This analysis revealed that the OR between HLA-A and total protein was 0.967 (95% CI: 0.948–0.987,  $P_{\text{fdr}} = 1.15\text{E-}02$ ). The results confirmed no horizontal pleiotropy between HLA-A and MASLD (MR-Egger intercept =  $-0.011$ ,  $P_{\text{fdr}} = 0.556$ ). The scatter plots and leave-one-out sensitivity analyses for the relationship between HLA-A and total protein are presented in Supplementary Figure 10. Further mediation analysis showed that total protein exhibited a significant mediating effect in the association between HLA-A and MASLD (Fig. 4A, B). Specifically, the total effect was 0.969 (95% CI: 0.960–0.979,  $P_{\text{fdr}} = 1.81 \times 10^{-6}$ ), with total protein mediating 23.61% of the relationship between HLA-A and MASLD (OR = 0.993,  $P_{\text{fdr}} < 0.05$ ).

### **Validation of the relationship between serum total protein levels and MASLD**

The independent validation cohort included 330 patients with MASLD confirmed by vibration-controlled transient elastography and 85 controls. Baseline characteristics of the participants are shown in Supplementary Table 3. In the

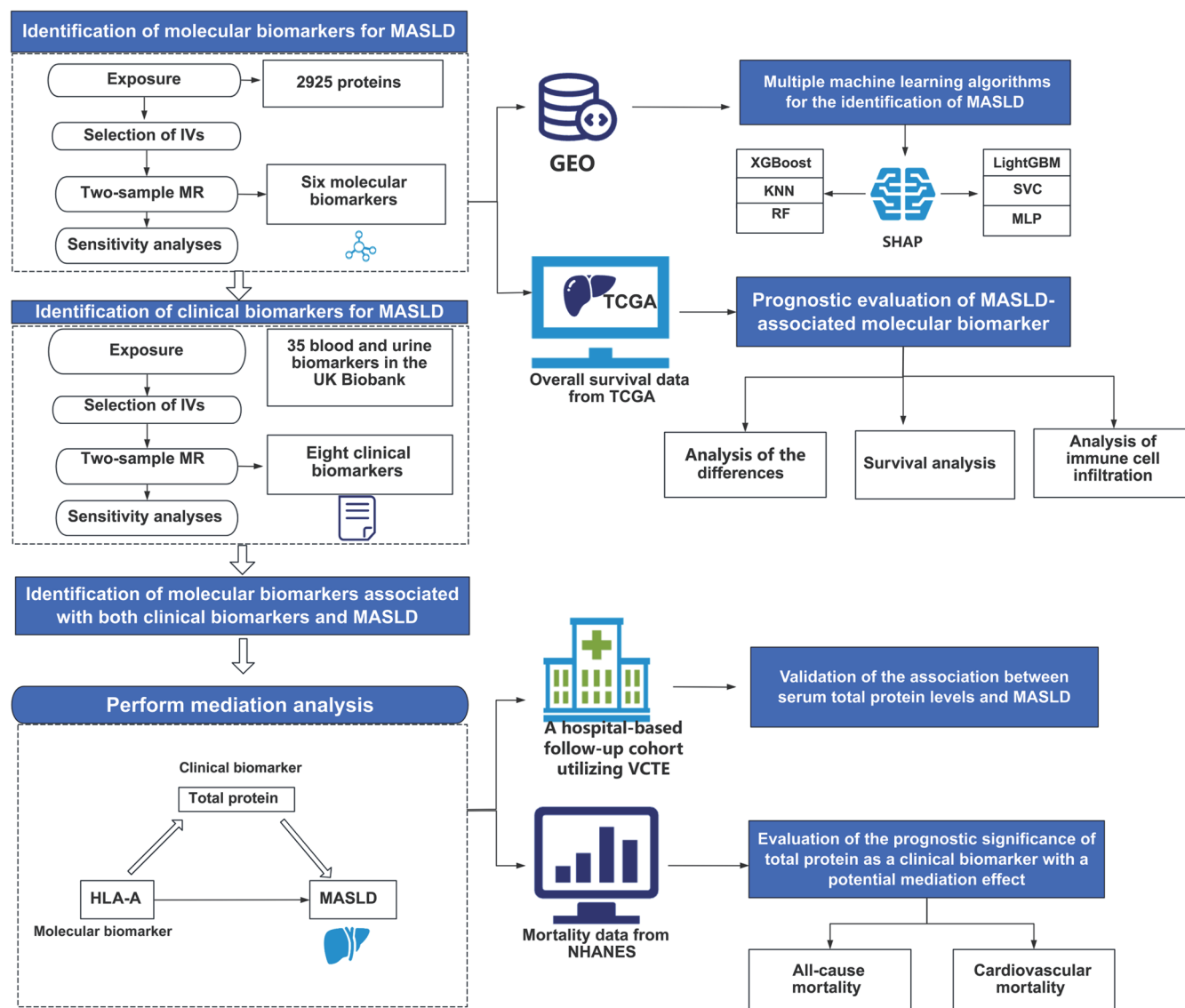


**Fig. 1. Flowchart of the study.** First, we conducted MR analysis to identify six molecular biomarkers and eight clinical biomarkers causally associated with MASLD. Mediation analysis was performed to determine whether key clinical biomarkers mediate the effects of molecular biomarkers (exposures) on MASLD (outcome). We found that total protein demonstrated a significant mediating effect in the relationship between HLA-A and MASLD. The association between total protein and MASLD was also externally validated in a hospital-based cohort. Second, we applied six machine learning algorithms to develop and validate a novel noninvasive diagnostic model for MASLD based on the identified molecular biomarkers. Third, we explored the prognostic value of molecular biomarkers for the development of, and poorer survival from, HCC by analyzing data from TCGA. We also evaluated the prognostic value of key clinical biomarkers for all-cause and cause-specific mortality by analyzing prospective data from the NHANES. HCC, hepatocellular carcinoma; MR, mendelian randomization; MASLD, metabolic dysfunction-associated steatotic liver disease; GEO, Gene Expression Omnibus; TCGA, The Cancer Genome Atlas; VCTE, vibration-controlled transient elastography; HLA-A, human leukocyte antigen A; NHANES, National Health and Nutrition Examination Survey.

subsequent multivariable logistic regression analysis (Supplementary Table 4), serum total protein levels showed a positive association with MASLD risk that remained statistically significant across all models. Specifically, in the age- and sex-adjusted model, the OR for MASLD was 1.103 (95% CI: 1.064–1.143). In multivariable model 1, which adjusted for age, sex, body mass index, diabetes, and hypertension, the OR was 1.092 (95% CI: 1.052–1.134,  $P < 0.001$ ). Even after additional adjustment for serum liver enzymes, lipids, creatinine, HbA1c, and platelet count (adjusted model 2), the association between total protein and MASLD remained significant, with an adjusted OR of 1.080 ( $P = 0.023$ ).

#### **Performance of multiple machine learning algorithms for MASLD based on six molecular biomarkers**

We developed a non-invasive model for diagnosing MASLD using the six identified molecular biomarkers and six commonly used supervised machine-learning algorithms. As shown in Figure 5A, the RF model demonstrated the best performance in the training set, achieving an AUC of 0.941 (95% CI: 0.829–1.000), followed by KNN (AUC = 0.885, 95% CI: 0.732–1.000) and XGBoost (AUC = 0.834, 95% CI: 0.662–0.975). Conversely, the MLP model performed poorly, with an AUC of 0.536 (95% CI: 0.244–0.827). Additionally, we applied the Shapley Additive exPlanations method to ana-

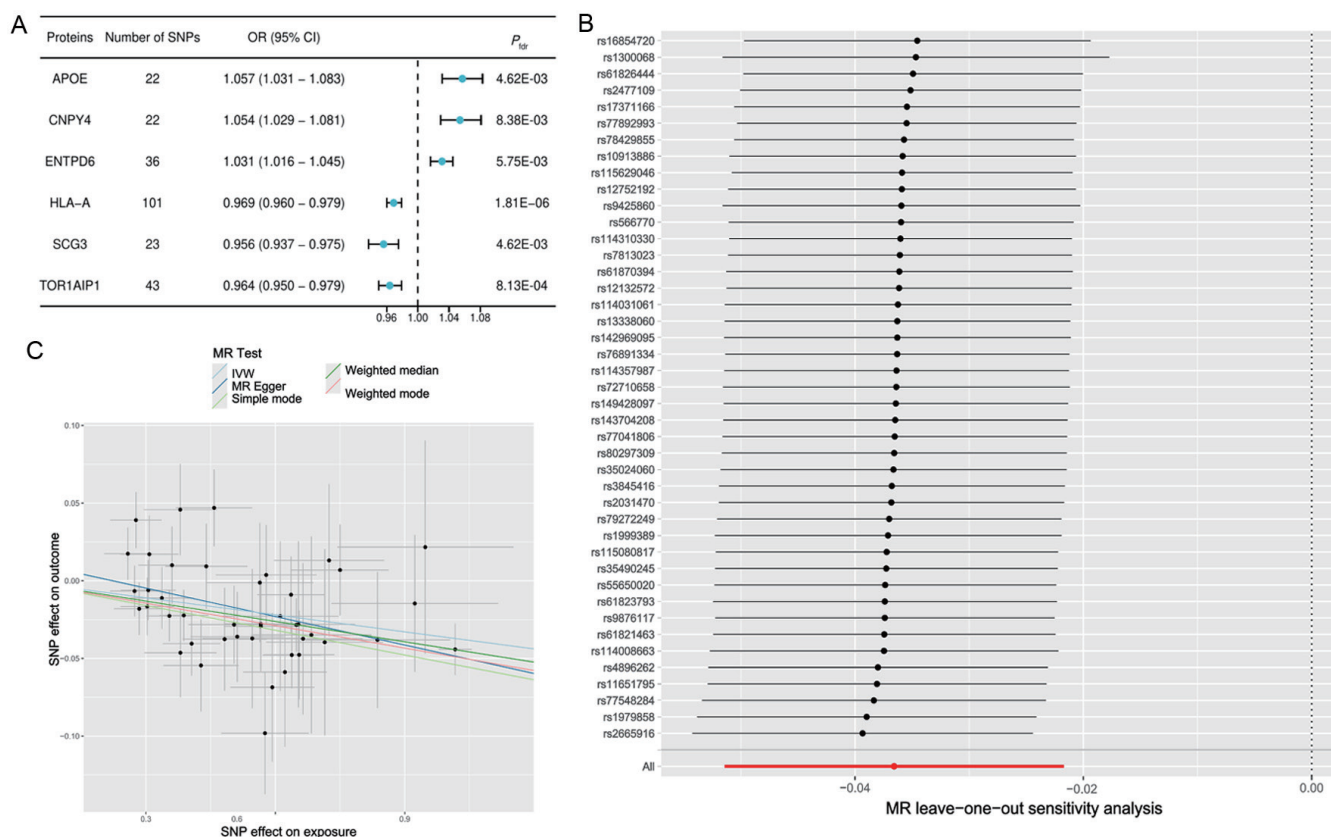


**Fig. 2. Causal molecular biomarkers related to MASLD.** (A) Forest plot displaying the causal effect estimates for six molecular biomarkers significantly associated with MASLD based on the IVW method; (B) Leave-one-out sensitivity analysis plot for TOR1AIP1; (C) Scatter plot of SNP effects on TOR1AIP1 (exposure) and MASLD (outcome). APOE, apolipoprotein E; CNPY4, canopy FGF signaling regulator 4; ENTPD6, ectonucleoside triphosphate diphosphohydrolase 6; HLA-A, major histocompatibility complex, class I, A; MR, mendelian randomization; MASLD, metabolic dysfunction-associated steatotic liver disease; OR, odds ratio; SCG3, secretogranin III; SNP, single nucleotide polymorphism; TCGA, The Cancer Genome Atlas; TOR1AIP1, torsin family 1 member A interacting protein 1; VCTE, vibration-controlled transient elastography; IVW, inverse variance weighted.

lyze the random forest model. As illustrated in Figure 5B, this analysis revealed that CNPY4, SCG3, TOR1AIP1, and ENTPD6 were the top four molecular features influencing the model output. Notably, CNPY4 exhibited the highest mean Shapley Additive exPlanations value, indicating its pivotal role in distinguishing MASLD from non-MASLD individuals. In the validation dataset (GSE48452) (Fig. 5C), the RF model maintained superior discriminative performance with an AUC of 0.875, demonstrating robust generalization and discriminative capability. KNN and XGBoost also showed consistent performance, while MLP continued to exhibit poor performance in the validation set (GSE48452). To assess the robustness and potential overfitting of the RF model, we performed 500 bootstrap resampling iterations separately in both the training and validation sets. The resulting ROC curves with 95% confidence intervals are shown in Supplementary Figure 11.

**Prognostic molecular and clinical biomarkers associated with MASLD**

We further analyzed the prognostic significance of key molecular biomarkers closely associated with MASLD, particularly their impact on the development of HCC and overall survival. We found that CNPY4 was significantly upregulated in HCC (Supplementary Fig. 12). Across multiple cancer types, elevated CNPY4 expression demonstrated varying degrees of association with overall survival, with a particularly strong

link in LIHC, where high CNPY4 expression was significantly associated with poor prognosis (HR = 1.753, Supplementary Fig. 13). Notably, in LIHC, CNPY4 expression was positively correlated with several immune cell types, especially macrophages, dendritic cells, and T helper cells (Supplementary Fig. 14), suggesting that CNPY4 may contribute to tumor progression by modulating the tumor immune microenvironment. Similarly, we observed that ENTPD6 was significantly overexpressed in LIHC ( $P < 0.001$ , Supplementary Fig. 15). Survival analysis indicated that high ENTPD6 expression was significantly associated with poorer overall survival in patients (HR = 1.483,  $P < 0.05$ , Supplementary Fig. 16), highlighting ENTPD6 as another potential adverse prognostic biomarker. In LIHC, ENTPD6 expression also exhibited significant positive associations with various immune cell populations, including dendritic cells, macrophages, CD8<sup>+</sup> T cells, T helper cells, and regulatory T cells ( $P < 0.05$ , Supplementary Fig. 17).

Given that serum total protein level mediates the effect of the molecular biomarker HLA-A on MASLD, we regarded it as an important clinical biomarker. Therefore, we further investigated its prognostic significance using data from the NHANES study. A total of 41,474 individuals were initially identified from the NHANES database. After excluding participants with missing data for serum total protein levels and mortality, 3,540 individuals were included in the final analysis. Kaplan–Meier survival curves are shown in Figure 6. In-

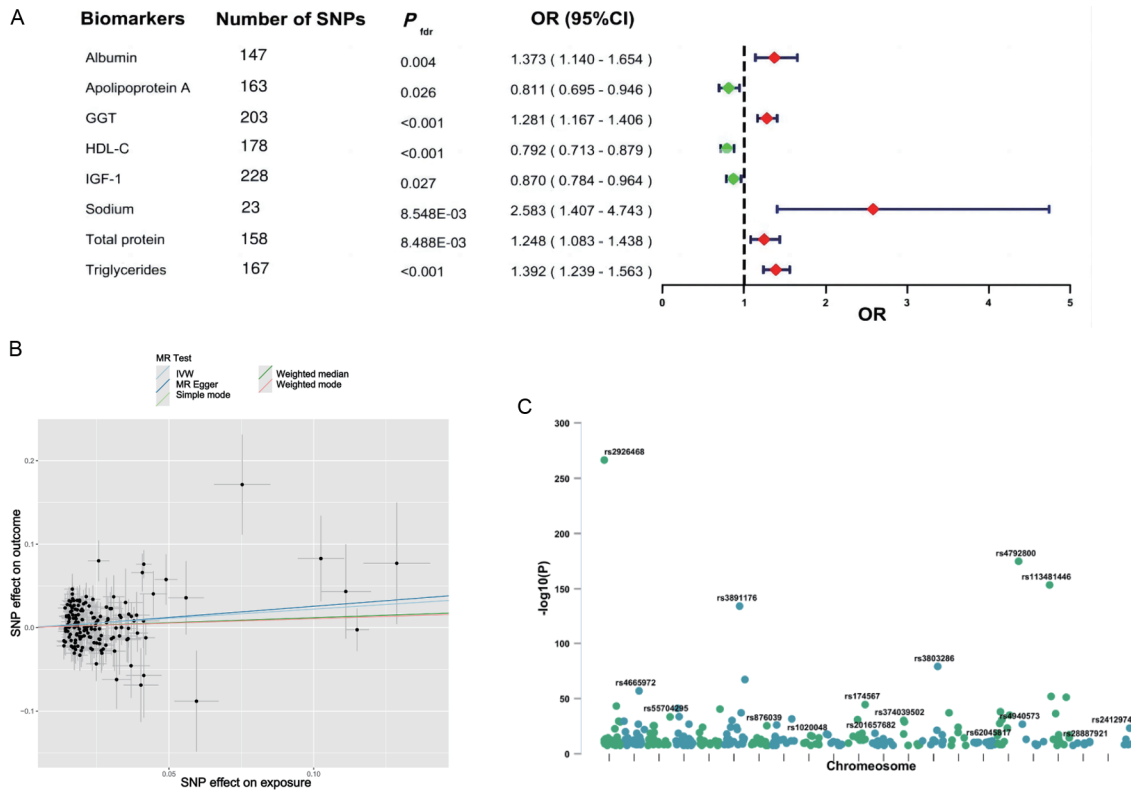


**Fig. 3. MR analysis revealing causal relationships between clinical biomarkers and MASLD.** (A) Forest plot displaying the causal effect estimates for eight clinical biomarkers significantly associated with MASLD. (B) Scatter plot showing the MR analysis for total protein as exposure and MASLD as the outcome. (C) Manhattan plot illustrating the distribution of SNPs associated with total protein across chromosomes. The  $-\log_{10}(P)$  values are plotted against chromosomal positions, highlighting genome-wide significant SNPs after linkage disequilibrium clumping. OR, Odds ratio; CI, Confidence interval; SNP, Single nucleotide polymorphism; MR, Mendelian randomization; IVW, Inverse variance weighting; GGT, Gamma-glutamyl transferase; HDL-C, High-density lipoprotein cholesterol; IGF-1, Insulin-like growth factor 1; MASLD, metabolic dysfunction-associated steatotic liver disease.

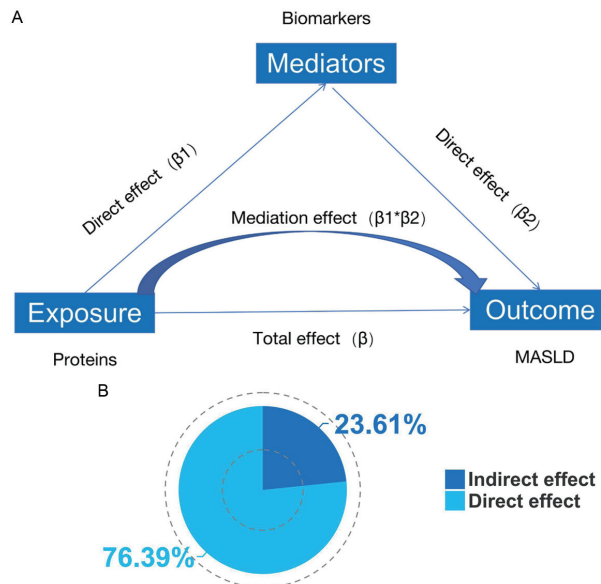


**Fig. 4. Mediation analysis exploring the role of total protein in the association between HLA-A and MASLD.** (A) Conceptual framework of the mediation analysis. Exposure (proteins) influences the outcome (MASLD) through direct and indirect pathways. The indirect effect is mediated by clinical biomarkers (mediators), while the direct effect bypasses the mediators. The total effect ( $\beta$ ) is the sum of the direct effect ( $\beta_2$ ) and the mediation effect ( $\beta_1 \times \beta_2$ ). (B) Proportion of the mediation and direct effects for the relationship between HLA-A, total protein, and MASLD. The indirect effect mediated by total protein accounts for 23.61% of the total association, whereas the direct effect contributes 76.39%. MASLD, metabolic dysfunction-associated steatotic liver disease; HLA-A, major histocompatibility complex, class I, A.

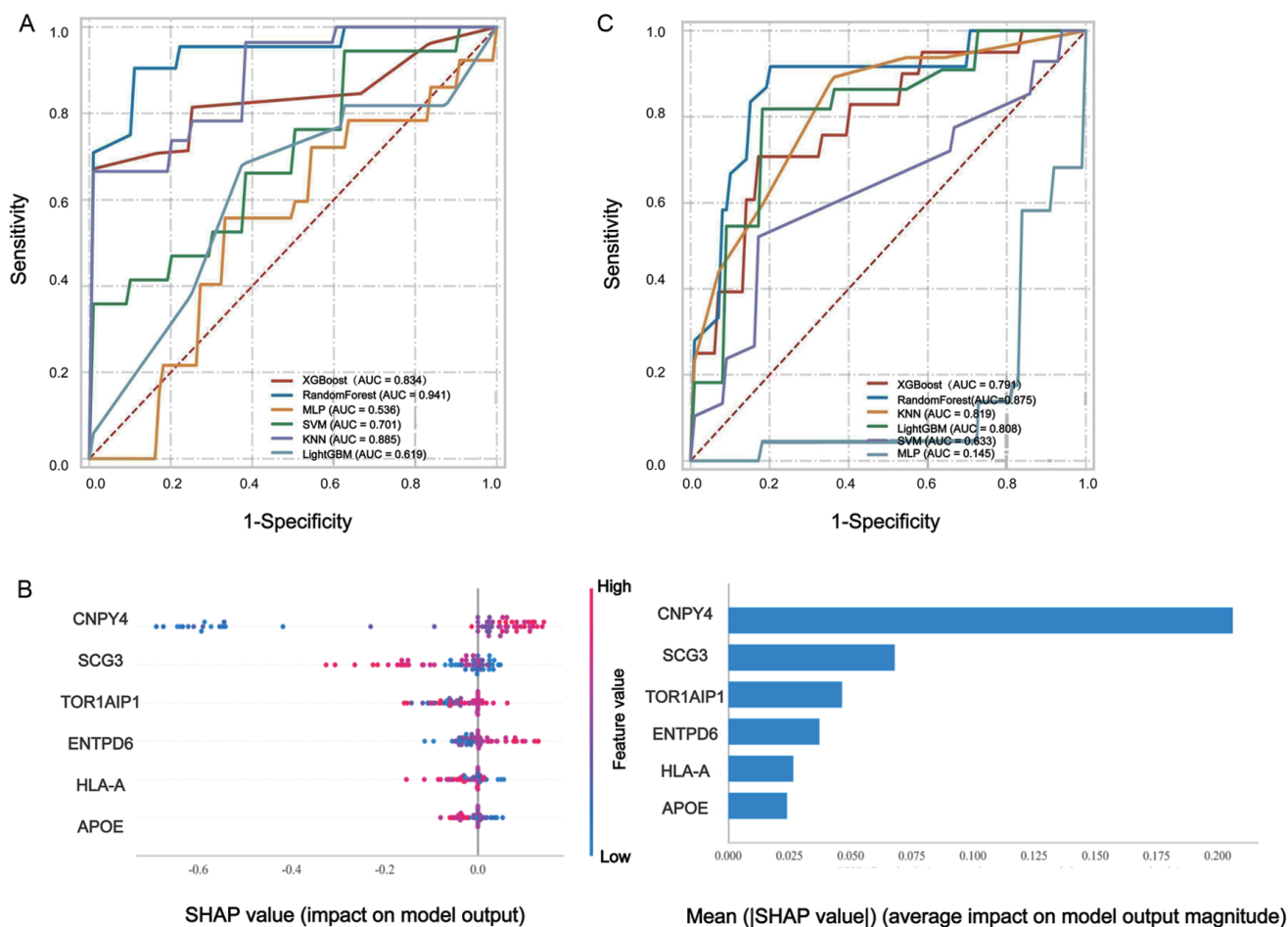


**Fig. 5. Performance evaluation and feature importance interpretation of machine learning models.** (A) ROC curves of six machine learning algorithms in the training set. (B) Feature importance analysis using SHAP. (C) ROC curves of the six machine learning models in the independent validation set. AUC, Area under the curve; ROC, Receiver operating characteristic; SVM, Support vector machine; LASSO, Least absolute shrinkage and selection operator; XGBoost, Extreme gradient boosting; SHAP, SHapley additive explanations; GGT, Gamma-glutamyl transferase; HDL-C, High-density lipoprotein cholesterol; APOE, Apolipoprotein E; CNPY4, Canopy FGF signaling regulator 4; SCG3, Secretogranin III; TOR1AIP1, Torsin family 1 member A interacting protein 1; ENTPD6, ectonucleoside triphosphate diphosphohydrolase 6; HLA-A, Major histocompatibility complex, class I, A.

dividuals with total protein levels < 60 g/L had a significantly higher risk of all-cause mortality compared to those with levels ≥ 60 g/L (HR = 2.180; 95% CI: 1.188–4.002) in the age- and sex-adjusted model. The HR was 2.769 (95% CI: 1.441–5.319) in regression model 1, which was adjusted for age, sex, marital status, hypertension, diabetes, and body mass index, and an HR of 2.495 (95% CI: 1.224–5.087) in regression model 2, which was additionally adjusted for serum GGT, ALT, total cholesterol, triglycerides, and platelet count (Supplementary Table 5).

### Discussion

In this study, we identified several molecular and clinical biomarkers causally associated with MASLD and explored their diagnostic significance for MASLD as well as their prognostic relevance for mortality outcomes. Notably, total serum protein levels were found to partially mediate the effect of HLA-A on the risk of MASLD, revealing a novel immunometabolic causal pathway. To translate these findings into a practical clinical tool, we developed a non-invasive diagnostic model based on the six MR-identified proteins using multiple

machine learning algorithms. Among these, the RF model demonstrated excellent performance (AUC = 0.941 in the training set and 0.875 in the validation set), underscoring its potential utility in early MASLD screening and diagnosis. Additionally, we demonstrated that higher expression levels of CNPY4 and ENTPD6 were associated with poorer overall survival in HCC, while lower serum total protein levels were linked to increased all-cause mortality in the general population. These findings suggest that certain MASLD-related biomarkers may have prognostic relevance in broader clinical settings.

In our study, six proteins (molecular biomarkers) were identified as having a significant causal relationship with MASLD. APOE is an essential component of chylomicrons, and studies have shown that polymorphisms in the *APOE* gene are closely related to MASLD development.<sup>22</sup> Amzolini and colleagues reported that the frequency of HLA-A25 in patients with MASLD was significantly lower than in healthy controls.<sup>23</sup> Shin *et al.* found that deletion of the *TOR1AIP1* gene induced MASLD development.<sup>24</sup> Currently, few reports exist on the associations of CNPY4, ENTPD6, and SCG3 with MASLD, and these proteins may represent key targets for

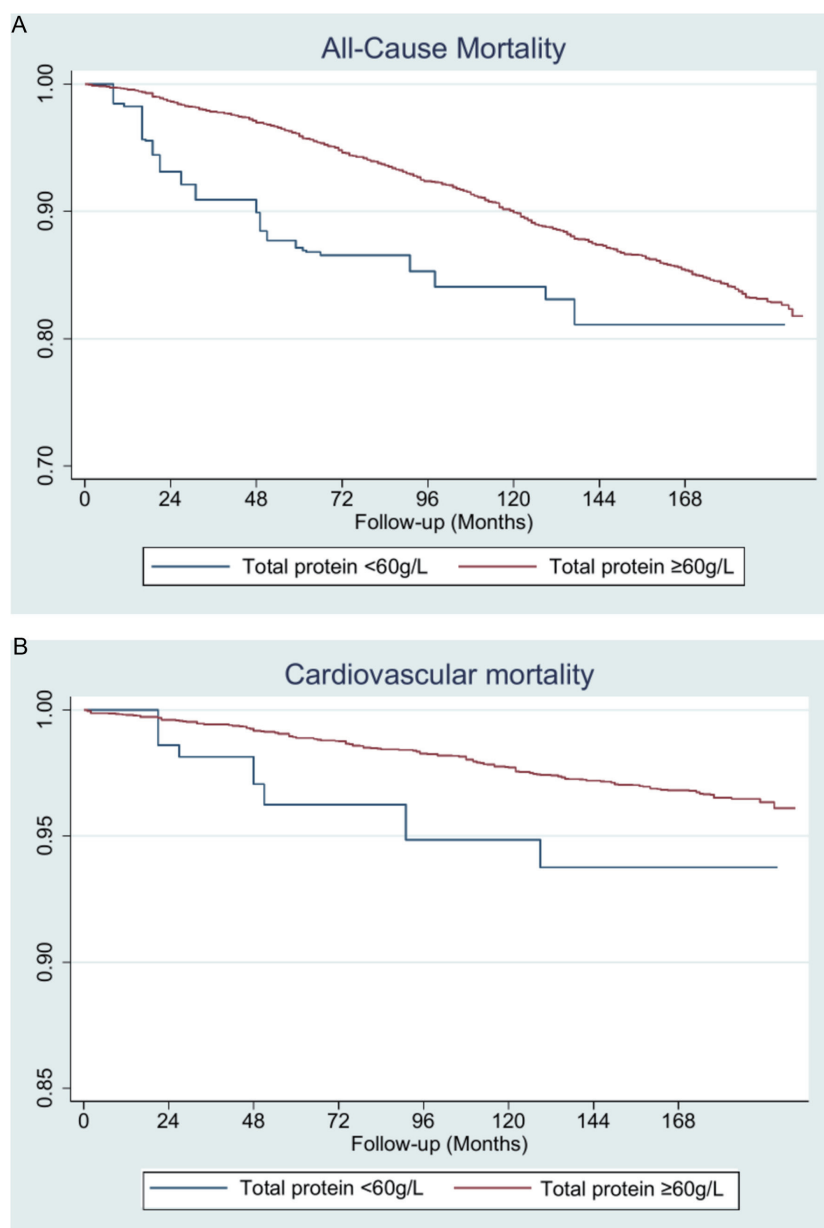


**Fig. 6. Kaplan–Meier survival curves for all-cause and cardiovascular mortality stratified by serum total protein levels (<60 g/L vs. ≥60 g/L).** (A) Kaplan–Meier survival curve for all-cause mortality stratified by serum total protein levels (<60 g/L vs. ≥60 g/L). (B) Kaplan–Meier survival curve for cardiovascular mortality stratified by serum total protein levels (<60 g/L vs. ≥60 g/L).

future research. CNPY4 is localized in the endoplasmic reticulum and assists in protein maturation and lipid synthesis. Hotta *et al.* found that the rs3764220 variant in the SCG3 gene was associated with metabolic syndrome.<sup>25</sup> ENTPD6 belongs to the ectonucleoside triphosphate diphosphohydrolase family; its encoded proteins hydrolyze nucleoside triphosphates and diphosphates, playing a crucial role in cell signaling and energy metabolism.<sup>26</sup> A recent MR study identified potential targets for abdominal obesity and found that ENTPD6 may be a novel biomarker for interventions targeting visceral adipose tissue.<sup>27</sup>

Among 35 blood and urine biomarkers, eight were identified as closely associated with MASLD. A meta-analysis of 12 studies revealed that circulating IGF-1 levels were sig-

nificantly lower in individuals with MASLD than in healthy controls.<sup>28</sup> GGT in human serum primarily originates from the liver and biliary system. Serum GGT level serves not only as a conventional liver function marker but also plays a broader role in metabolic health.<sup>29</sup> Additionally, serum GGT is included in the fatty liver index equation used to identify hepatic steatosis.<sup>30</sup> Furthermore, urinary sodium concentration was closely associated with MASLD (OR = 2.48, 95% CI: 1.52–4.06).<sup>31</sup>

HLA-A is a member of the major histocompatibility complex class I family and plays a central role in antigen presentation and immune surveillance. Genetic variations in HLA-A have previously been associated with metabolic and inflammatory diseases.<sup>32–34</sup> This study revealed that total protein functions

as a (partial) mediator in the causal pathway from HLA-A to MASLD, accounting for 23.61% of the total effect. Our mediation analysis indicates that downregulation of HLA-A may lead to increased total protein levels, which in turn could elevate MASLD risk. The liver is enriched with CD4<sup>+</sup> T helper cells, CD8<sup>+</sup> cytotoxic T cells, and B lymphocytes, all contributing to persistent inflammation and tissue remodeling.<sup>35,36</sup> Mechanistically, HLA-A, a core component of MHC class I molecules, is responsible for presenting endogenous antigens to CD8<sup>+</sup> T cells, thereby maintaining immune surveillance and homeostasis. When HLA-A expression is reduced, impaired antigen presentation leads to dysfunctional CD8<sup>+</sup> T-cell activation and inefficient clearance of endogenous antigens derived from apoptotic cells or lipotoxic stress.<sup>37,38</sup> The persistence of these antigens may induce chronic antigenic stimulation, activate B cells, and promote polyclonal immunoglobulin production, resulting in elevated serum globulin and thus increased total protein.<sup>39</sup> The consequent elevation in globulin contributes to increased total protein concentrations, indicative of immune activation, which plays a crucial role in MASLD pathogenesis and progression.<sup>40</sup> These findings suggest that HLA-A downregulation may indirectly contribute to MASLD by promoting immune pathways.

In this study, six ML algorithms were used to construct a noninvasive MASLD diagnostic model. The application of ML in MASLD has made remarkable progress in recent years, positioning it as a pivotal tool for precise diagnosis and treatment.<sup>41</sup> ML broadly includes supervised, unsupervised, semi-supervised, and reinforcement learning based on training methods.<sup>42</sup> In our analysis, we used supervised ML and found that RF had the best discriminative power, outperforming other algorithms. RF is an ensemble learning algorithm based on decision trees, which significantly improves model accuracy by integrating predictions from multiple decision trees.<sup>43</sup> Compared with other algorithms, RF has better tolerance for noise and outliers because its prediction results are based on synthesizing multiple decision trees.<sup>44</sup> Furthermore, RF demonstrates resistance to overfitting and strong generalization abilities through its randomized construction approach.<sup>43</sup>

Previous studies have shown that patients with MASLD are at increased risk of developing HCC.<sup>45</sup> In our study, we found that CNPY4 and ENTPD6 not only contribute to the pathogenesis of MASLD but may also play a role in HCC development, further supporting their significance and utility as molecular biomarkers related to liver disease. Moreover, both CNPY4 and ENTPD6 were associated with poor prognosis in HCC, suggesting their potential as prognostic biomarkers in liver diseases. CNPY4 is closely associated with immune regulation and exhibits carcinogenic effects across various tumors.<sup>46</sup> ENTPD6 is involved in extracellular purine metabolism and may contribute to tumor metabolic reprogramming by modulating mitochondrial function. Previous studies have consistently demonstrated that the rs738409 variant in the PNPLA3 gene, which encodes patatin-like phospholipase domain-containing protein 3, significantly increases the risk of both MASH and MASLD-related HCC.<sup>47,48</sup> This variant impairs triglyceride hydrolysis in hepatocytes, promoting lipid accumulation and resulting in more than a twofold increase in MASH risk (compared to healthy controls) and a 2.2-fold increased risk of MASLD-related HCC (compared to MASLD patients without the variant).<sup>47,48</sup> However, as a static genetic susceptibility variant, PNPLA3 is primarily useful for long-term risk prediction and does not reflect dynamic biological changes during disease progression. In contrast, CNPY4 and ENTPD6 are expression-based protein biomarkers that can be quantitatively monitored and may offer greater potential

for clinical translation, particularly in dynamic risk stratification, progression surveillance, and therapeutic response assessment in MASLD-HCC.

Additionally, based on prospective data from the NHANES study, we found that individuals with serum total protein levels below 60 g/L, a marker identified as a potential mediator of mortality, exhibited an increased risk of all-cause mortality. This may be because hypo-proteinemia often reflects inadequate protein intake or synthesis, leading to malnutrition, impaired organ function, delayed tissue repair, and reduced resilience to illness. Hypo-proteinemia can also result in edema, ascites, hypovolemia, and tissue hypoperfusion, potentially triggering complications such as renal dysfunction and hypotension, all of which may contribute to increased all-cause mortality.<sup>49</sup>

Although this study employed the MR method, it has several limitations. First, the GWAS data lack extensive validation across different ethnic groups. Therefore, future studies must validate these findings in diverse populations to confirm the causal relationships. Second, while we identified causal proteins and biomarkers associated with MASLD, the specific biological mechanisms underlying these findings remain unexplored. Third, MASLD is a metabolically driven liver disease with complex and multifactorial etiologies. Other potential mediators, particularly those related to systemic inflammation or immune-metabolic interactions, may exist but were not included in the current analysis due to limitations in the available datasets. Future studies incorporating more comprehensive inflammatory markers, multi-omics data, and immune phenotyping are warranted to refine and expand the mediation pathway models. Fourth, the hospital-based cohort used in this study was derived from a tertiary medical center and had a relatively limited sample size, which may introduce selection bias. Compared with the general MASLD population, patients treated at tertiary centers are more likely to have complex disease presentations and a higher burden of metabolic comorbidities. Such differences in population characteristics may affect the generalizability of our findings.

## Conclusions

We identify six causal molecular biomarkers (e.g., CNPY4, ENTPD6, HLA-A) and eight clinical biomarkers (e.g., serum total protein) for MASLD across various independent cohorts. Serum total protein levels partially mediated the effect of HLA-A on MASLD, highlighting a novel immune-metabolic pathway. Based on these findings, we develop a random forest model that demonstrates high accuracy in identifying MASLD. Additionally, CNPY4 and ENTPD6 are associated with poor survival in HCC, while low serum total protein levels predicted higher all-cause mortality. These findings support a multi-omics framework for biomarker-driven diagnosis and risk prediction in MASLD.

## Acknowledgments

We would like to acknowledge all participants and investigators involved in the FinnGen study. CDB is supported in part by the Southampton National Institute for Health and Care Research, Biomedical Research Centre (NIHR203319). We would like to express our heartfelt gratitude to Dr. Xue-Liang Yang and Dr. Xiao-Cheng Li for their invaluable suggestions.

## Funding

This work was supported by the Key Research and Develop-

ment Program of the Shaanxi Provincial Department of Science and Technology (2025GH-YBXM-032), the Project of the Shaanxi Provincial Administration of Traditional Chinese Medicine (2022-SLRH-YQ-011), the Tianjin Key Medical Discipline (Specialty) Construction Project (TJYXZDXK-077D), the Natural Science Basic Research Program of Shaanxi (2023-JC-QN-0949) and the National Inheritance Studio Project of Zheng Qinglian (Document No. [2022] 270).

### Conflict of interest

CDB has received grant support from Echosens. GT has been an Editorial Board Member of *Journal of Clinical and Translational Hepatology* since 2018, MHZ has been an Associate Editor of *Journal of Clinical and Translational Hepatology* since 2013. The other authors have no conflict of interests related to this publication.

### Author contributions

Study design, data interpretation, and verification (FY, GF, NH), data analysis and collection (GF, NH), writing of the manuscript (GF, FY, NH, MHZ, GT, CDB, YL, HZ, MM), and revision (MHZ, GT, CDB, YL, HZ, MM, FY). All authors reviewed and commented on the manuscript and approved the final version.

### Ethical statement

The study was conducted in accordance with the Declaration of Helsinki (as revised in 2024) and approved by the Ethics Committee of the First Affiliated Hospital of Xi'an Medical University (approval number: XYFY2018LSK-003). The writing informed consent was waived for retrospective analysis.

### Data sharing statement

The data supporting the findings of this study are available from the corresponding author upon reasonable request.

### References

- Younossi ZM, Golabi P, Paik JM, Henry A, Van Dongen C, Henry L. The global epidemiology of nonalcoholic fatty liver disease (NAFLD) and nonalcoholic steatohepatitis (NASH): a systematic review. *Hepatology* 2023;77(4):1335–1347. doi:10.1097/HEP.0000000000000004, PMID:36626630.
- Le P, Tatar M, Dasarathy S, Alkhoury N, Herman WH, Taksler GB, *et al*. Estimated Burden of Metabolic Dysfunction-Associated Steatotic Liver Disease in US Adults, 2020 to 2050. *JAMA Netw Open* 2025;8(1):e2454707. doi:10.1001/jamanetworkopen.2024.54707, PMID:39821400.
- Ioannou GN. Epidemiology and risk-stratification of NAFLD-associated HCC. *J Hepatol* 2021;75(6):1476–1484. doi:10.1016/j.jhep.2021.08.012, PMID:34453963.
- Huang H, Liu Z, Xu M, Chen Y, Xu C, Wang L, Wang N. Global burden trends of MAFLD-related liver cancer from 1990 to 2019. *Portal Hypertens Cirrhosis* 2023;2(4):157–164. doi:10.1002/poh2.63.
- Polyzos SA, Chrysavgis L, Vachliotis ID, Chartampilas E, Cholongitas E. Nonalcoholic fatty liver disease and hepatocellular carcinoma: Insights in epidemiology, pathogenesis, imaging, prevention and therapy. *Semin Cancer Biol* 2023;93:20–35. doi:10.1016/j.semcancer.2023.04.010, PMID:37149203.
- Huang DQ, Wong VWS, Rinella ME, Boursier J, Lazarus JV, Yki-Järvinen H, *et al*. Metabolic dysfunction-associated steatotic liver disease in adults. *Nat Rev Dis Primers* 2025;11(1):14. doi:10.1038/s41572-025-00599-1, PMID:40050362.
- Xia T, Du M, Li H, Wang Y, Zha J, Wu T, *et al*. Association between Liver MRI Proton Density Fat Fraction and Liver Disease Risk. *Radiology* 2023;309(1):e231007. doi:10.1148/radiol.231007, PMID:37874242.
- Yuan M, Hu X, Yao L, Chen P, Wang Z, Liu P, *et al*. Causal Relationship Between Gut Microbiota and Liver Cirrhosis: 16S rRNA Sequencing and Mendelian Randomization Analyses. *J Clin Transl Hepatol* 2024;12(2):123–133. doi:10.14218/JCTH.2023.00259, PMID:38343609.
- Xu S, Liu L, Li C, Ren Y, Zhang M, Xiang L, *et al*. Correlation Among Psoriasis, Iridocyclitis, and Non-alcoholic Fatty Liver Disease: Insights from Mendelian Randomization and Mediation Analysis. *Int J Med Sci*

- 2025;22(1):121–131. doi:10.7150/ijms.102369, PMID:39744174.
- Yan X, Huang S, Li H, Feng Z, Kong J, Liu J. The causal effect of mTORC1-dependent circulating protein levels on nonalcoholic fatty liver disease: A Mendelian randomization study. *Dig Liver Dis* 2024;56(4):559–564. doi:10.1016/j.dld.2023.09.017, PMID:37778897.
- Di Mauro S, Scamporrino A, Filippello A, Di Pino A, Scicali R, Malaguerma R, *et al*. Clinical and Molecular Biomarkers for Diagnosis and Staging of NAFLD. *Int J Mol Sci* 2021;22(21):11905. doi:10.3390/ijms222111905, PMID:34769333.
- Du Y, Li R, Fu D, Zhang B, Cui A, Shao Y, *et al*. Multi-omics technologies and molecular biomarkers in brain tumor-related epilepsy. *CNS Neurosci Ther* 2024;30(4):e14717. doi:10.1111/cns.14717, PMID:38641945.
- Trinks J, Mascardi MF, Gadano A, Marciano S. Omics-based biomarkers as useful tools in metabolic dysfunction-associated steatotic liver disease clinical practice: How far are we? *World J Gastroenterol* 2024;30(14):1982–1989. doi:10.3748/wjg.v30.i14.1982, PMID:38681130.
- Feng G, Zhang X, Zhang L, Liu WY, Geng S, Yuan HY, *et al*. Novel urinary protein panels for the non-invasive diagnosis of non-alcoholic fatty liver disease and fibrosis stages. *Liver Int* 2023;43(6):1234–1246. doi:10.1111/liv.15565, PMID:36924436.
- Wu XX, Zheng KI, Boursier J, Chan WK, Yilmaz Y, Romero-Gómez M, *et al*. acNASH index to diagnose nonalcoholic steatohepatitis: a prospective derivation and global validation study. *EClinicalMedicine* 2021;41:101145. doi:10.1016/j.eclinm.2021.101145, PMID:34646997.
- Feng G, Mózes FE, Ji D, Treprasertsuk S, Okanoue T, Shima T, *et al*. acFibroMASH index for the diagnosis of fibrotic MASH and prediction of liver-related events: An international multicenter study. *Clin Gastroenterol Hepatol* 2025;23(5):785–796. doi:10.1016/j.cgh.2024.07.045, PMID:39362618.
- Kurki MI, Karjalainen J, Palta P, Sipilä TP, Kristiansson K, Donner KM, *et al*. FinnGen provides genetic insights from a well-phenotyped isolated population. *Nature* 2023;613(7944):508–518. doi:10.1038/s41586-022-05473-8, PMID:36653562.
- Sinnott-Armstrong N, Tanigawa Y, Amar D, Mars N, Benner C, Aguirre M, *et al*. Genetics of 35 blood and urine biomarkers in the UK Biobank. *Nat Genet* 2021;53(2):185–194. doi:10.1038/s41588-020-00757-z, PMID:33462484.
- Ghodsian N, Abner E, Emdin CA, Gobeil É, Taba N, Haas ME, *et al*. Electronic health record-based genome-wide meta-analysis provides insights on the genetic architecture of non-alcoholic fatty liver disease. *Cell Rep Med* 2021;2(11):100437. doi:10.1016/j.xcrm.2021.100437, PMID:34841290.
- Feng G, He N, Gao J, Li XC, Zhang FN, Liu CC, *et al*. Causal relationship between key genes and metabolic dysfunction-associated fatty liver disease risk mediated by immune cells: A Mendelian randomization and mediation analysis. *Diabetes Obes Metab* 2024;26(12):5590–5599. doi:10.1111/dom.15925, PMID:39228284.
- Lin H, Lee HW, Yip TC, Tsochatzis E, Petta S, Bugianesi E, *et al*. Vibration-Controlled Transient Elastography Scores to Predict Liver-Related Events in Steatotic Liver Disease. *JAMA* 2024;331(15):1287–1297. doi:10.1001/jama.2024.1447, PMID:38512249.
- Liu S, Weng R, Gu X, Li L, Zhong Z. Association between apolipoprotein E gene polymorphism and nonalcoholic fatty liver disease in Southern China: A case-control study. *J Clin Lab Anal* 2021;35(12):e24061. doi:10.1002/jcla.24061, PMID:34664321.
- Amzolini AM, Fortofoiu M, Tudorica-Micu SE, Fortofoiu MC, Neagoe D, Popescu M, *et al*. Genetic Factors Involved in the Development and Progression of Nonalcoholic Fatty Liver Disease. *Curr Health Sci J* 2015;41(4):297–301. doi:10.12865/CHSJ.41.04.01, PMID:30538833.
- Shin JY, Hernandez-Ono A, Fedotova T, Östlund C, Lee MJ, Gibeley SB, *et al*. Nuclear envelope-localized torsinA-LAP1 complex regulates hepatic VLDL secretion and steatosis. *J Clin Invest* 2019;129(11):4885–4900. doi:10.1172/JCI129769, PMID:31408437.
- Hotta K, Kitamoto T, Kitamoto A, Mizusawa S, Matsuo T, Nakata Y, *et al*. Association of variations in the FTO, SCG3 and MTMR9 genes with metabolic syndrome in a Japanese population. *J Hum Genet* 2011;56(9):647–651. doi:10.1038/jhg.2011.74, PMID:21796137.
- Zimmermann H. Ectonucleoside triphosphate diphosphohydrolases and ecto-5'-nucleotidase in purinergic signaling: how the field developed and where we are now. *Purinergic Signal* 2021;17(1):117–125. doi:10.1007/s11302-020-09755-6, PMID:33336318.
- Zhang G, Han B, Chen Y, Jiang W, Fu J, Xu X, *et al*. Genetic insights into visceral obesity with health conditions, from disease susceptibility to therapeutic intervention. *Postgrad Med J* 2025. doi:10.1093/postmj/qgaf004, PMID:39835424.
- Yao Y, Miao X, Zhu D, Li D, Zhang Y, Song C, *et al*. Insulin-like growth factor-1 and non-alcoholic fatty liver disease: a systemic review and meta-analysis. *Endocrine* 2019;65(2):227–237. doi:10.1007/s12020-019-01982-1, PMID:31243652.
- Kwak J, Seo IH, Lee YJ. Serum  $\gamma$ -glutamyltransferase level and incidence risk of metabolic syndrome in community dwelling adults: longitudinal findings over 12 years. *Diabetol Metab Syndr* 2023;15(1):29. doi:10.1186/s13098-023-01000-5, PMID:36823659.
- Chung GE, Jeong SM, Cho EJ, Yoo JJ, Cho Y, Lee KN, *et al*. Association of fatty liver index with all-cause and disease-specific mortality: A nationwide cohort study. *Metabolism* 2022;133:155222. doi:10.1016/j.metabol.2022.155222, PMID:35636583.
- Shojaei-Zarghani S, Safarpour AR, Fattahi MR, Keshtkar A. Sodium in relation with nonalcoholic fatty liver disease: A systematic review and meta-analysis of observational studies. *Food Sci Nutr* 2022;10(5):1579–1591. doi:10.1002/fsn3.2781, PMID:35592291.
- Zhang J, Zhao L, Wang B, Gao J, Wang L, Li L, *et al*. HLA-A\*33-DR3 and A\*33-DR9 haplotypes enhance the risk of type 1 diabetes in Han Chi-

- nese. *J Diabetes Investig* 2016;7(4):514–521. doi:10.1111/jdi.12462, PMID:27181214.
- [33] Jin H, Kim YA, Lee Y, Kwon SH, Do AR, Seo S, *et al*. Identification of genetic variants associated with diabetic kidney disease in multiple Korean cohorts via a genome-wide association study mega-analysis. *BMC Med* 2023;21(1):16. doi:10.1186/s12916-022-02723-4, PMID:36627639.
- [34] Karrar A, Hariharan S, Fazel Y, Moosvi A, Houry M, Younoszai Z, *et al*. Analysis of human leukocyte antigen allele polymorphism in patients with non alcoholic fatty liver disease. *Medicine (Baltimore)* 2019;98(32):e16704. doi:10.1097/MD.00000000000016704, PMID:31393374.
- [35] Li Z, Wang S, Xu Q, Su X, Wang Y, Wang L, *et al*. The double roles of T cell-mediated immune response in the progression of MASLD. *Biomed Pharmacother* 2024;173:116333. doi:10.1016/j.biopha.2024.116333, PMID:38479177.
- [36] Li H, Xia N. The multifaceted roles of B lymphocytes in metabolic dysfunction-associated steatotic liver disease. *Front Immunol* 2024;15:1447391. doi:10.3389/fimmu.2024.1447391, PMID:39372417.
- [37] Dhatchinamoorthy K, Colbert JD, Rock KL. Cancer Immune Evasion Through Loss of MHC Class I Antigen Presentation. *Front Immunol* 2021;12:636568. doi:10.3389/fimmu.2021.636568, PMID:33767702.
- [38] Sari G, Rock KL. Tumor immune evasion through loss of MHC class-I antigen presentation. *Curr Opin Immunol* 2023;83:102329. doi:10.1016/j.coi.2023.102329, PMID:37130455.
- [39] Ahmed R, Ford ML, Sanz I. Regulation of T and B cell responses to chronic antigenic stimulation during Infection, autoimmunity and transplantation. *Immunol Rev* 2019;292(1):5–8. doi:10.1111/imr.12836, PMID:31883175.
- [40] Jee YM, Lee JY, Ryu T. Chronic Inflammation and Immune Dysregulation in Metabolic-Dysfunction-Associated Steatotic Liver Disease Progression: From Steatosis to Hepatocellular Carcinoma. *Biomedicines* 2025;13(5):1260. doi:10.3390/biomedicines13051260, PMID:40427086.
- [41] Zhu G, Song Y, Lu Z, Yi Q, Xu R, Xie Y, *et al*. Machine learning models for predicting metabolic dysfunction-associated steatotic liver disease prevalence using basic demographic and clinical characteristics. *J Transl Med* 2025;23(1):381. doi:10.1186/s12967-025-06387-5, PMID:40155991.
- [42] Sarker IH. Machine Learning: Algorithms, Real-World Applications and Research Directions. *SN Comput Sci* 2021;2(3):160. doi:10.1007/s42979-021-00592-x, PMID:33778771.
- [43] Feng G, Zheng KI, Li YY, Rios RS, Zhu PW, Pan XY, *et al*. Machine learning algorithm outperforms fibrosis markers in predicting significant fibrosis in biopsy-confirmed NAFLD. *J Hepatobiliary Pancreat Sci* 2021;28(7):593–603. doi:10.1002/jhbp.972, PMID:33908180.
- [44] Feng G, He N, Xia HH, Mi M, Wang K, Byrne CD, *et al*. Machine learning algorithms based on proteomic data mining accurately predicting the recurrence of hepatitis B-related hepatocellular carcinoma. *J Gastroenterol Hepatol* 2022;37(11):2145–2153. doi:10.1111/jgh.15940, PMID:35816347.
- [45] Kong Q, Kong D, Li B, Peng W, Chen Z. Impact of Metabolic Dysfunction-Associated Fatty/Steatotic Liver Disease on Hepatocellular Carcinoma Incidence and Long-Term Prognosis Post-Liver Resection: A Systematic Review and Meta-Analysis. *Acad Radiol* 2025. doi:10.1016/j.acra.2025.01.003, PMID:39843280.
- [46] Li JW, Huang QR, Mo LG. CNPY4 is a potential promising prognostic-related biomarker and correlated with immune infiltrates in gliomas. *Medicine (Baltimore)* 2022;101(33):e30044. doi:10.1097/MD.00000000000030044, PMID:35984129.
- [47] Anstee QM, Darlay R, Cockell S, Meroni M, Govaere O, Tiniakos D, *et al*. Genome-wide association study of non-alcoholic fatty liver and steatohepatitis in a histologically characterised cohort. *J Hepatol* 2020;73(3):505–515. doi:10.1016/j.jhep.2020.04.003, PMID:32298765.
- [48] Liu YL, Patman GL, Leathart JB, Piguet AC, Burt AD, Dufour JF, *et al*. Carriage of the PNPLA3 rs738409 C >G polymorphism confers an increased risk of non-alcoholic fatty liver disease associated hepatocellular carcinoma. *J Hepatol* 2014;61(1):75–81. doi:10.1016/j.jhep.2014.02.030, PMID:24607626.
- [49] Tan Y, Xiang W, Chen Y, Huang J, Sun D. Effect of hypoproteinemia on mortality of elderly male patients with chronic heart failure. *Medicine (Baltimore)* 2024;103(5):e37078. doi:10.1097/MD.00000000000037078, PMID:38306508.